Journal of Alloys and Compounds 504S (2010) S368–S371

Contents lists available at ScienceDirect

Journal of Alloys and Compounds

journal homepage: www.elsevier.com/locate/jallcom

Epitaxial growth of self-arranged periodic ZnO nanostructures on sapphire substrates grown by MOCVD

Hou-Guang Chen [a,*], Sheng-Rui Jian [a], Zheng-Wei Li [a], Kuan-Wei Chen [b], Jhih-Cheng Li [a]

[a] Department of Materials Science and Engineering, I-Shou University, Kaohsiung 840, Taiwan
[b] Department of Mechanical Engineering, National Cheng Kung University, Tainan 701, Taiwan

ARTICLE INFO

Article history:
Received 2 July 2009
Received in revised form 28 January 2010
Accepted 27 February 2010
Available online 7 March 2010

Keywords:
ZnO
Nanostructure
XRD
TEM
Epitaxial growth

ABSTRACT

This article reports an investigation on the growth behaviour of ZnO epitaxial nanostructures and thin films grown by metalorganic chemical vapour deposition (MOCVD). Self-arranged periodic ZnO nanostructures consisting of a large number of ZnO nano-columns can be directly grown on bare sapphire surface without any lithography or other pre-patterning processes. The spacing of periodic nanostructures was ~117 nm. The measurements of XRD $2\theta/\omega$ and φ scans indicated that epitaxial and non-epitaxial ZnO grains coexisted on the same substrate. According to cross-sectional transmission electron microscopy observation, these periodic ZnO nanostructures were epitaxially grown on sapphire substrates and separated by non-epitaxial ZnO grains. However, the in-plane periodic arrangement of ZnO nanostructures disappeared while increasing the growth temperature. Initial sapphire surface structure and CVD growth kinetics closely relate to the growth of self-arranged periodic ZnO nanostructures.

1. Introduction

One-dimensional ZnO nanostructures have been received extensively interest due to their fascinating physical properties, including wide band gap (3.36 eV), high exciton binding energy at room temperature (60 meV), piezoelectrisity, extraordinary structural diversity, and chemical-sensing effect [1–4]. Therefore, various novel applications in electronics, optoelectronics and electromechanical nanodevices have demonstrated, such as nanolasers [1,5], nanowire-field transistors [6], solar cells [7], and piezo-nanogenerators [2]. A regular spatial organization of ZnO nanostructures is necessary for the realization of above-mentioned nanodevices. Thus, many attempts to make significant advance in the control of spatial position, density, and morphology of ZnO nanostructures have been devoted by numerous groups, and various methods have been proposed to achieve spatial organization of ZnO nanostructures, including electron-beam lithography [8], self-assembled nanosphere array templates [9], and nano-imprint technologies [10].

Epitaxial growth has been regarded as a key technology for advanced optoelectronic device applications. Recently, various self-organized III-V semiconductor nanostructures can be successfully obtained through heteroepitaxial growth processes [11]. While a wide range of substrates have been used for growing high quality ZnO epitaxial thin film and nanostructures [12–15], sapphire is more favored substrate for the epitaxial growth of ZnO thin films or nanostructures, owing to low cost and large size single-crystal being commercially available. In this article, we show that self-arranged periodic striped ZnO nanostructures can be directly grown on the (0 0 0 1) plane sapphire surface by controlling CVD growth kinetic and substrate surface structure without any complicated lithographies or sophisticated processes. The mechanism of the growth of self-arranged periodic ZnO nanostructures on sapphire is proposed and discussed.

2. Experimental procedure

A reduced pressure hot-wall type MOCVD apparatus was employed to implement the epitaxial growth of ZnO nanostructures on *c*-plane sapphire substrates. Zinc acetylacetonate ($Zn(acac)_2$, 99.995 purity) and O_2 (99.999 purity) were used as the zinc and oxygen source, respectively. The precursor of $Zn(acac)_2$ was heated at 90 °C before introduction into the chamber by carrier gas of nitrogen (99.99%), which was separated from oxygen flow before reaching the substrate surface to avoid to direct reaction of oxygen with zinc source. Prior to ZnO growth, as-received *c*-plane sapphire substrates in 1 cm × 1 cm size was annealed at 1200 °C in air for 4 h and then were ultrasonically cleaned by acetone. The ZnO nanostructures were grown at temperatures of 450 and 500 °C, respectively, for 120 min.

X-ray diffraction characterization of ZnO nanostructures was carried out by a Philips X'Pert diffractometer with a Cu Kα radiation source. The field emission scanning electron microscopy (FESEM, Hitachi S-4700) and atomic force microscopy (AFM, Digital Instrument: NanoMan NS4+D3100) were used to examine the topography of ZnO nanostructures and sapphire surface, respectively. Cross-sectional transmission electron microscopy (XTEM) observation was performed on a Philips

* Corresponding author at: Department of Materials Science and Engineering, I-Shou University, No. 1, Sec. 1, Syuecheng Rd., Dashu Township, Kaohsiung 840, Taiwan. Tel.: +886 7 6577711x3113; fax: +886 7 6578444.
E-mail address: houguang@isu.edu.tw (H.-G. Chen).

0925-8388/$ – see front matter © 2010 Elsevier B.V. All rights reserved.
doi:10.1016/j.jallcom.2010.02.195

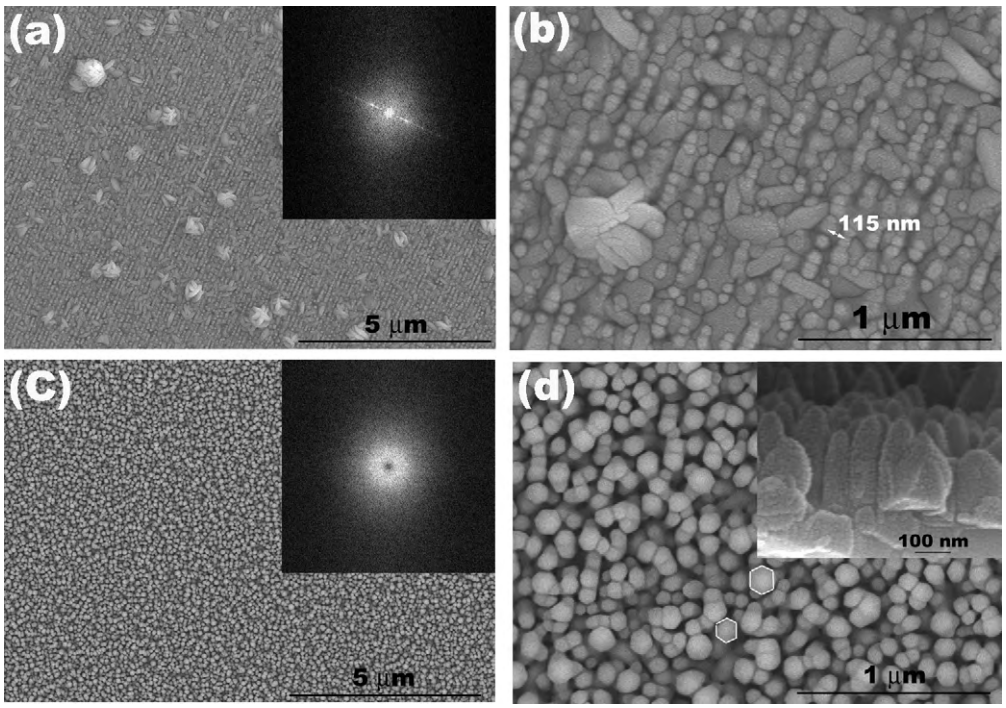

Fig. 1. Low and high magnification of SEM images of the ZnO nanostructures grown at the different temperatures: ((a) and (b)) 450 °C, ((c) and (d)) 500 °C. The insets in (a) and (c) showing the corresponding FFT power spectra obtained from the SEM images. The inset in (d) showing the corresponding cross-sectional SEM image.

Tecnai G2 microscope operated at 200 kV. The site-specific cross-sectional XTEM specimen was prepared by focused ion beam technique (FIB).

3. Results and discussion

Fig. 1 shows SEM images of ZnO nanostructures grown at the different growth temperatures. It is interesting to note that periodic striped nanostructures can be found in the sample grown at 450 °C, as shown in Fig. 1(a). Furthermore, the periodicity of the striped nanostructures can be deduced from the fast Fourier transformation (FFT) power spectrum of the SEM image (the inset of Fig. 1(a)). The FFT power spectrum exhibits a set of sharp spots, indicating that the striped ZnO nanostructures have high degree of spatial ordering, which corresponds to the spatial periodicity of 117 nm. According to the enlarged SEM image of Fig. 1(a), a large number of dot-like ZnO grains with an average size of about 60 nm lining-up to form striped nanostructures along a specific direction are clearly shown in Fig. 1(b). The measured spacing between two adjacent striped nanostructures is approximately 115 nm, which is in good agreement with the FFT results. In addition to striped nanostructures, irregularly shaped grains which are recognized as polycrystalline ZnO grains can be seen from the image. However, in the case of ZnO nanostructures deposited at the temperature of 500 °C, ZnO nanorods with diameters of ~100 nm grew over the entire sample, as shown in Fig. 1(c) and (d). The corresponding FFT spectrum (inset of Fig. 1(c)) exhibits a broad ring around the origin of Fourier space, suggesting that the ZnO nanorods distribute randomly on the substrate without any spatial ordering. In Fig. 1(d), the top faces of ZnO nanorods appear to hexagonal in shape, as marked by white lines, indicating that [0 0 0 1] direction of these ZnO nanorods are parallel to the sample normal direction. Vertically aligned ZnO nanorods grown over the sample can be further verified by cross-sectional SEM observation (the inset of Fig. 1(d)).

Fig. 2 shows the XRD $2\theta/\omega$ spectra of the ZnO nanostructures grown at the temperatures of 450 and 500 °C, respectively. Both of XRD spectra display strongly (0 0 0 l) family reflections of ZnO, suggesting that the ZnO nanostructures present a c-axis preferred orientation. However, the $2\theta/\omega$ scan obtained from ZnO grown at 450 °C, a weak peak corresponding to ZnO ($10\bar{1}1$) reflection appears in the spectrum. The irregularly shaped polycrystalline grains which have been observed in Fig. 1(b) might contribute to this weak diffraction peak.

The in-plane crystallographic relationship between ZnO nanostructures and sapphire substrates was established using the XRD φ-scan shown in Fig. 3. The ZnO ($11\bar{2}2$) and sapphire ($11\bar{2}6$) planes were used to perform the φ-scan measurements. In Fig. 3(a), the φ-scan for the ($11\bar{2}2$) reflection of ZnO grown at 450 °C exhibits sixfold symmetry with a rotation of 30° with respect to sapphire, indicating that a large portion of ZnO nanostructures formed on c-plane sapphire substrate exhibits in-plane align-

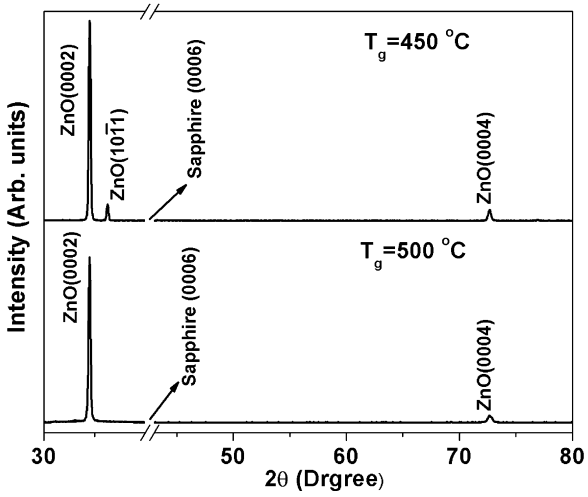

Fig. 2. XRD $2\theta/\omega$ scans corresponding to the ZnO nanostructures grown at 450 and 500 °C.

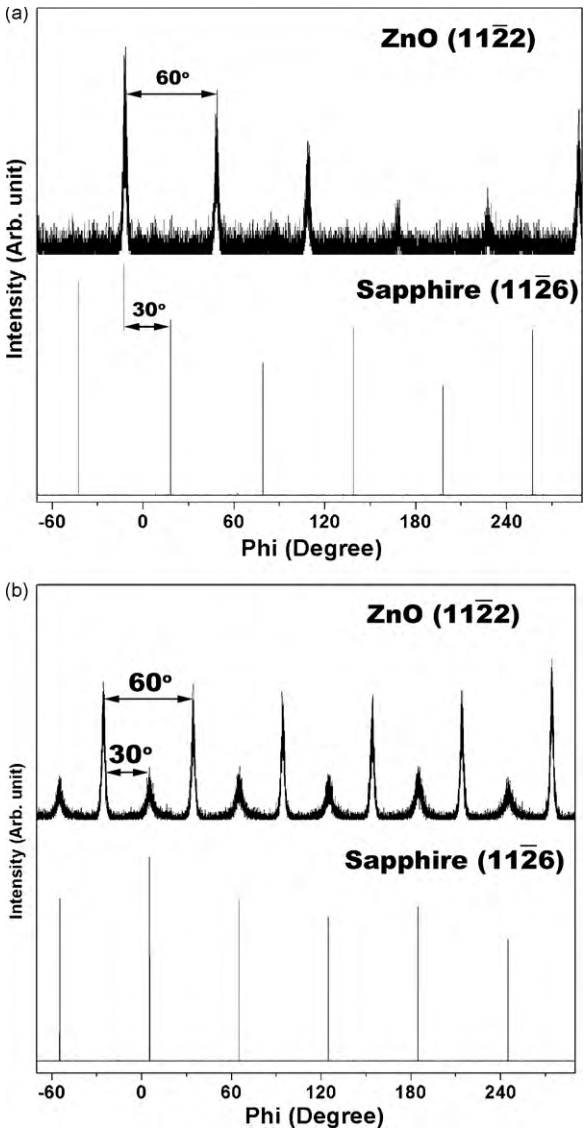

Fig. 3. XRD φ-scans of ZnO $\{1\,1\,\bar{2}\,2\}$ and sapphire $\{1\,1\,\bar{2}\,6\}$ reflections corresponding to the ZnO nanostructures grown at (a) 450 °C and (b) 500 °C.

ment following the relationship of $(0\,0\,0\,1)_{ZnO}||(0\,0\,0\,1)_{sapphire}$ and $[1\,1\,\bar{2}\,0]_{ZnO}||[1\,0\,\bar{1}\,0]_{sapphire}$, although the existence of polycrystalline ZnO grains have been detected from SEM observation and XRD $2\theta/\omega$ analysis. In contrast, two sets of peaks with an angle difference of 30° coexist in the φ-scan profile of ZnO nanorods grown at 500 °C, as shown in Fig. 3(b). The other set of peaks, as marked by stars, is regarded as well-known 30° rotation domains with an in-plane orientation of $[1\,0\,\bar{1}\,0]_{ZnO}||[1\,0\,\bar{1}\,0]_{sapphire}$. These two kinds of in-plane orientation relationship between ZnO and sapphire are often observed in ZnO epitaxially grown on *c*-plane sapphire substrates [16,17].

In order to directly observe the periodic striped ZnO nanostructures grown on sapphire substrate, characterization of XTEM was performed, which is essential for understanding the growth mechanism. A thin foil specimen for XTEM observation was extracted from an elongated area across several ZnO nano-stripes by site-specific FIB milling and ex situ pick-up techniques. In Fig. 4(a), the bright field XTEM image shows that several column-like ZnO grains with rounded tip, as indicated by black arrows, embedded in ZnO layer exhibit dark contrast. Note that the mean distance between adjacent rounded ZnO columns ranges from 100 to 120 nm, which is similar to the periodicity of striped nanostructures. Thus, these well-separated rounded ZnO columns correlate to the dot-like ZnO grains which line-up to form striped nanostructures, as seen in the SEM images (Fig. 1(b)). A selected area electron diffraction (SAED) pattern (inset of Fig. 4(a)), was taken from an interface between ZnO column and sapphire along the zone axis of sapphire $[1\,\bar{2}\,1\,0]$ direction. The result of diffraction pattern definitely indicates the epitaxial growth of rounded ZnO columns on sapphire and the epitaxial relationship between nano-columns and substrate as follows $(0\,0\,0\,1)_{ZnO}||(0\,0\,0\,1)_{sapphire}$ and $[1\,1\,\bar{2}\,0]_{ZnO}||[1\,0\,\bar{1}\,0]_{sapphire}$. In Fig. 4(b), all rounded ZnO columns are in contrast in the dark-field image obtained by using the ZnO 0 0 0 2 diffraction spot to image; however, other regions between two adjacent ZnO columns are out-of-contrast, indicating that these periodic striped ZnO

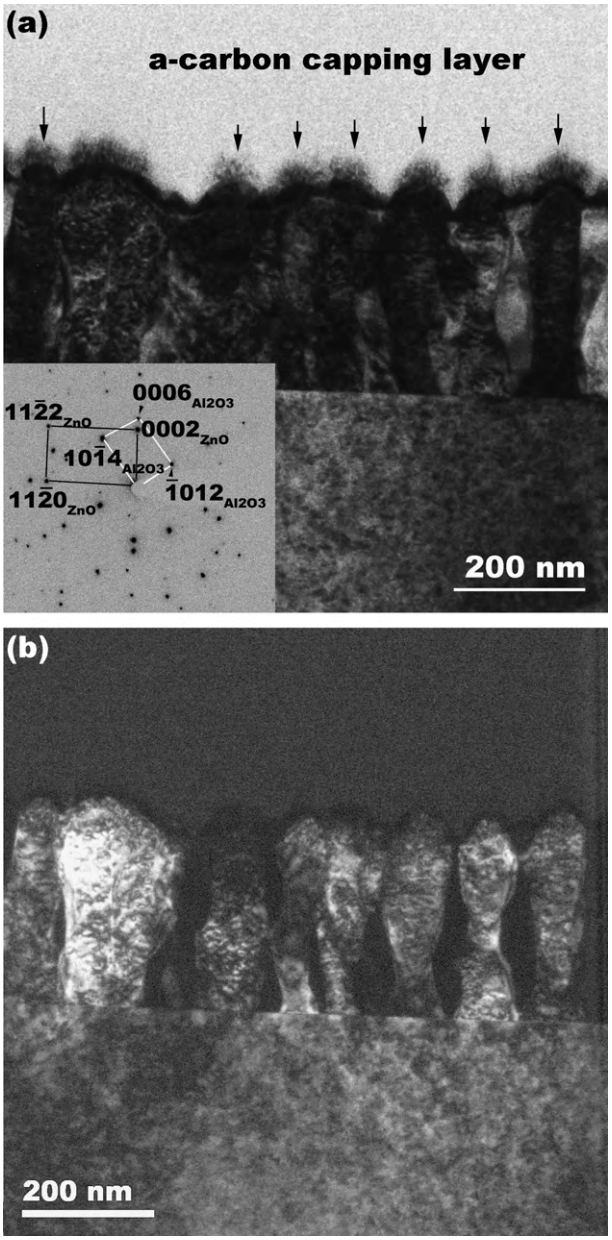

Fig. 4. (a) XTEM bright field image of a FIB milled foil extracted from an elongated area across several ZnO nano-stripes showing several rounded column grains with dark contrast, as indicated by black arrows. The insert in (a) showing corresponding SEAD pattern taken from the interface region between ZnO nano-column and sapphire substrate. (b) XTEM dark-field image obtained by using ZnO 0 0 0 2 diffraction spot to image.

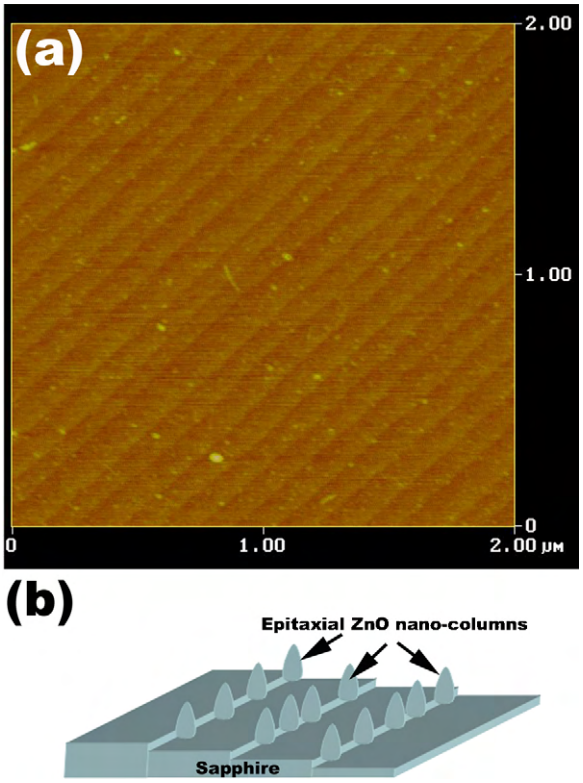

Fig. 5. (a) AFM image (2 μm × 2 μm area) of the as-annealed sapphire surface. (b) The schematic illustration of self-arranged epitaxial ZnO nano-columns grown along the linear step edges.

nanostructures were epitaxially grown on sapphire substrate and separated by non-epitaxial crystalline materials.

In this work, the periodic striped ZnO nanostructures were directly grown on sapphire substrate without any lithography process. The exact reason is not known as to why the self-arranged periodic ZnO nanostructures can be formed on the bare sapphire substrate, but a preliminary inference can be given by considering sapphire surface structure. Thus, AFM was employed to clarify the correlation between the periodic arrangement of self-organized ZnO nanostructures and sapphire surface structure. In Fig. 5(a) the AFM image (2 μm × 2 μm area) of as-annealed sapphire surface displays a linear step and terrace structure, which exhibits periodically faceted structure. Noting that the terrace-width distribution ranging from 100 to 120 nm is in the same range with the periodicity of striped ZnO nanostructures, and hence the growth of periodic ZnO nanostructures is closely related to such periodically faceted surface structure. In general, such step edges which have a large number of dangling bonds act as preferred nucleation sites for heteroepitaxial growth. Therefore, periodically faceted surface of sapphire provides a natural template for the epitaxial growth of self-arranged periodic nanostructures. The linearly aligned ZnO nanodots arrays grown along the step edges of sapphire by MOCVD have also been reported in other literatures [18,19]. In present case, the linear step edges act as nucleation sites for epitaxial growth of self-arranged periodic ZnO nano-columns, as illustrated in Fig. 5(b). In addition, based on the dark-field TEM observation, non-epitaxial crystalline materials were also grown on the substrate. The relatively low growth temperature (450 °C) is possibly responsible for the formation of non-epitaxial ZnO grains. Furthermore, the absence of non-epitaxial ZnO grains can be found as increasing growth temperature, which was confirmed by XRD measurements ($2\theta/\omega$- and φ-scans). However, the in-plane periodic arrangement of nanostructures disappears while growing at 500 °C. The growth temperature is another important factor to the formation of self-arranged periodic ZnO nanostructures, because adsorption, diffusion, and desorption of adatoms on substrate surface during CVD process significantly depends on the growth temperature. The influence of the growth conditions on the formation of self-arranged periodic nanostructures is still not explicit at the moment and will be clarified in future work.

4. Conclusion

In this article, self-arranged periodic nanostructures consisting of epitaxial ZnO nano-columns have been directly grown on bare *c*-plane sapphire substrates by MOCVD without any pre-patterning processes. According to the results of XRD and TEM characterization, these periodic ZnO nanostructures were epitaxially grown on sapphire substrate following the relation of $(0\,0\,0\,1)_{ZnO}||(0\,0\,0\,1)_{sapphire}$ and $[1\,1\,\bar{2}\,0]_{ZnO}||[1\,0\,\bar{1}\,0]_{sapphire}$. The periodicity of ZnO nanostructure was closely related to the mean terrace-width which was verified by AFM observation. Periodically faceted surface of annealed sapphire provides a natural template for the epitaxial growth of self-organized periodic nanostructures. The growth of self-arranged periodic ZnO nanostructures significantly depends on the initial sapphire surface structure and CVD growth kinetics.

Acknowledgements

We thank the support from National Science Council, Taiwan, ROC and I-Shou University, under Grant Nos.: NSC97-2221-E-214-006, NSC98-2221-E-214-018, ISU97-S-04, NSC97-2112-M-214-002-MY2 and ISU 97-S-02.

References

[1] H.M. Huang, S. Mao, H. Feick, H.Q. Yan, Y.Y. Wu, H. Kind, E. Weber, R. Russo, P.D. Yang, Science 292 (2001) 1897.
[2] Z.L. Wang, J. Song, Science 312 (2006) 242.
[3] C.S. Dandeneau, Y.H. Jeon, C.T. Shelton, Thin Solid Films 517 (2009) 4448.
[4] L. Schmidt-Mende, J.L. MacManus-Driscoll, Mater. Today 10 (2007) 40.
[5] P.D. Yang, H.Q. Yan, S. Mao, R. Russo, J. Johnson, R. Saykally, N. Morris, J. Pham, R.R. He, H.J. Choi, Adv. Funct. Mater. 12 (2002) 323.
[6] M.S. Arnold, P. Avouris, Z.W. Pan, Z.L. Wang, J. Phys. Chem. B 107 (2003) 659.
[7] M. Law, L.E. Greene, J.C. Johnson, R. Saykally, P.D. Yang, Nat. Mater. 4 (2005) 455.
[8] S. Xu, Y. Wei, M. Kirkham, J. Liu, W. Mai, D. Davidovic, R.L. Snyder, Z.L. Wang, J. Am. Chem. Soc. 130 (2008) 14958.
[9] A. Rahm, M. Lorenz, T. Nobis, G. Zimmermann, M. Grundmann, B. Fuhrmann, F. Syrowatka, Appl. Phys. A 88 (2007) 31.
[10] C.H. Wang, A.S.W. Wong, G.W. Ho, Langmuir 23 (2007) 11960.
[11] R.S. Goldman, B. Shin, B. Lita, Phys. Stat. Sol. (a) 195 (2003) 151.
[12] J.M. Jang, C.R. Kim, H. Ryu, M. Razeghi, W.G. Jung, J. Alloys Compd. 463 (2008) 503.
[13] Y.C. Chao, C.W. Lin, D.J. Ke, Y.H. Wu, H.G. Chen, L. Chang, Y.T. Ho, M.H. Liang, J. Cryst. Growth 298 (2007) 461.
[14] T. Ive, T. Ben-Yaacov, C.G. Van de Walle, U.K. Mishra, S.P. DenBaars, J.S. Speck, J. Cryst. Growth 310 (2008) 3407.
[15] Z.Q. Zeng, Y.Z. Liu, H.T. Yuan, Z.X. Mei, X.L. Du, J.F. Jia, Q.K. Xue, Z. Zhang, Appl. Phys. Lett. 90 (2007) 081911.
[16] C. Liu, S.H. Chang, T.W. Noh, M. Abouzaid, P. Ruterana, H.H. Lee, D.W. Kim, J.S. Chung, Appl. Phys. Lett. 90 (2007) 011906.
[17] M. Ying, X. Du, Z. Mei, Z. Zeng, H. Zheng, Y. Wang, J. Jia, Z. Zhang, Q. Xue, J. Phys. D: Appl. Phys. 37 (2004) 3058.
[18] X. Zhou, S. Gu, F. Qin, S. Zhu, J. Ye, S. Liu, W. Liu, R. Zhang, Y. Shi, Y. Zheng, J. Cryst. Growth 269 (2004) 362.
[19] K. Kametani, H. Imamoto, S. Fujita, Physics E 32 (2006) 33.